With the Authors' Compliments

Shock Compression Experiments in Solids using High Explosives

Tsuneaki Goto, Yasuhiko Syono, Jun Nakai and Yasuaki Nakagawa

Reprinted from
the Science Reports of the Research Institutes,
Tôhoku University

SCI. REP. RITU, A-Vol. 25, No. 6

SENDAI, JAPAN

Nov., 1975

Shock Compression Experiments in Solids using High Explosives*

Tsuneaki GOTO, Yasuhiko SYONO, Jun NAKAI
and Yasuaki NAKAGAWA

The Research Institute for Iron, Steel and Other Metals

(Received June 23, 1975)

Synopsis

Small-scale explosive plane wave generators, 40–78 mm in diameter, are developed to perform solid state experiments at shock pressures up to 1 Mbar. Techniques for determining the shock compression curve are described in detail, especially in the case where a phase transformation occurs at a high pressure.

I. Introduction

Since a shock compression technique was first applied to determine the equation of state for various metals at Los Alamos Scientific Laboratory[1], the technique has extensively been used as a standard method to generate ultrahigh dynamic pressures extending to a few Mbar and to measure the equation of state for condensed matters. Until now, various new techniques[2],[3] have been developed to perform basic solid state experiments, such as electrical resistivity[4] and optical absorption measurements[5]. Moreover, flash X-ray diffraction studies[6],[7] during shock compression have recently been attempted to show that the crystal is transformed to the hydrostatically compressed state in spite of the uniaxial shock compression.

The present authors have developed some small-size explosive devices for production of plane shock wave to perform 'university-scale' shock experiments at pressures up to 1 Mbar[8],[9],[10]. A small-size plane wave generator has been

---

* The **1642nd** report of the Research Institute for Iron, Steel and Other Metals.

(1) M.H. Rice, R.G. McQueen and J.M. Walsh, in *Solid State Physics*, (F. Seitz and D. Turnbull, eds.) Vol. 6, Academic Press, (1958) p. 1.
(2) R.N. Keeler and E.B. Royce, in *Physics of High Energy Density*, (P. Caldirola and H. Knoepfel, eds.) Academic Press, (1971), p. 51.
(3) W.J. Murri, D.R. Curran, C.F. Pertersen and R.C. Crewdson, Poulter Laboratory Technical Report 001–71, Stanford Research Institute (1971).
(4) D.L. Styris and G.E. Duvall, High Temperatures-High Pressures, **2** (1970), 447.
(5) E.S. Gaffney and T.J. Ahrens, J. geophys. Res., **78** (1973), 5942.
(6) Q. Johnson, A.C. Mitchell and L. Evans, Appl. Phys. Lett., **21** (1972), 29.
(7) A.C. Mitchell, Q. Johnson and L. Evans, Adv. X-ray Anal. **16** (1973), 242.
(8) Y. Syono, T. Goto, J. Nakai, Y. Nakagawa and H. Iwasaki, J. Phys. Soc. Japan, **37** (1974), 442.
(9) Y. Syono, T. Goto, J. Nakai and Y. Nakagawa. Proceedings of the 4th International Conference on High Pressure, Kyoto (1974), 466.
(10) T. Goto, Y. Syono, J. Nakai and Y. Nakagawa, Submitted to Solid State Commun.

examined with a high-speed streak camera and proved to be quite satisfactory for practical use. Using this device, determinations of the equation of state and measurements of electrical resistivity have been performed on transition metal oxides and semiconducting III–V compounds.

In the present paper, explosive devices for production of plane shock waves are described in detail, together with several techniques of the shock compression experiments, after a brief summary of shock relations in the next section. The experiments have been performed at Michikawa Laboratory for Explosive Experiments at Iwaki-machi in Akita Prefecture.

II. Basic shock relations

When an ideal plane shock wave travels in a slab of compressible material, a uniformly compressed state is realized behind a shock front, as shown in Fig. 1. The initial undisturbed state and the final compressed state are denoted by subscripts 0 and 1, respectively. The shock of velocity U and pressure P_1 accelerates the material particles to a velocity u_1, causing a density increase from ρ_0 to ρ_1 and an internal energy increase from E_0 to E_1. In a short time Δt the shock front $\mathscr{S}$ travels a distance $U\Delta t$, while the material particles ahead of or behind the shock front travel a distance $u_0\Delta t$ or $u_1\Delta t$, respectively. Therefore the mass flowing in or out of the shock front of unit area during Δt is given by $\rho_0(U-u_0)\Delta t$ or $\rho_1(U-u_1)\Delta t$, which must be equal to each other:

$$\rho_0(U-u_0) = \rho_1(U-u_1)\,. \tag{1}$$

In the same way, the following shock relations[1],[11] are obtained from the conservation of mometum and energy across the shock front:

$$P_1-P_0 = \rho_0(U-u_0)(u_1-u_0)\,, \tag{2}$$

$$P_1(u_1-u_0) = \frac{1}{2}\rho_0(U-u_0)(u_1-u_0)^2+\rho_0(U-u_0)(E_1-E_0)\,. \tag{3}$$

Using eqs. (1) and (2), the shock compressed state, characterized by P_1 and ρ_1, is determined by the measurement of U and u_1. (Usually $u_0=0$ and $P_0=1$ bar.) A function $\rho_1(P_1)$ is called the Hugoniot equation of state or, for short, the Hugoniot.

Since a direct observation of the particle velocity u_1 is usually difficult, u_1 is indirectly obtained by the measurement of the free surface velocity u_f. At shock pressures up to 500 kbar, the assumption that $u_f\simeq 2u_1$ (the free surface approximation) has been found to be correct for most materials within an error of about 1%[1]. To obtain more accurate shock wave data, the impedance match method[12] is used: The shock state of the specimen placed on a standard material whose Hugoniot is well known can be determined by measuring only the shock velocities of both the

(11) G.E. Duvall and G.R. Fowles, in *High Pressure Physics and Chemistry*, (R.S. Bradley, ed.) Vol. 2, Academic Press, (1963), p. 209.

(12) J.M. Walsh and R.H. Christian, Phys. Rev., **97** (1955), 1544.

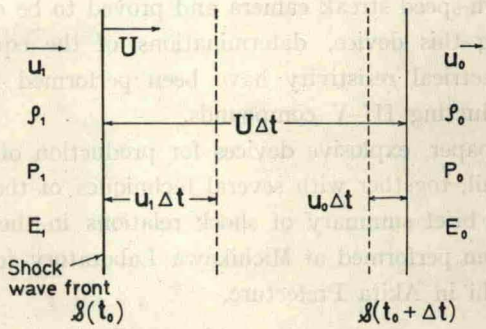

Fig. 1. Progress of a plane shock wave

specimen and the standard material. Usually a shock compressed state is determined by means of both the free surface approximation method and the impedance match method in order to check the experimental results.

Eliminating U and u_1 from eqs. (1)–(3), the increase of the internal energy due to the shock compression is expressed as

$$E_1-E_0=\frac{1}{2}(P_1+P_0)(V_0-V_1)\,, \tag{4}$$

where $V\equiv 1/\rho$. This equation, called the Rankine-Hugoniot relation,[1],[11] indicates that the shock compression differs from both the isothermal compression and the isentropic compression. The temperature increase due to the shock compression is in general larger than that due to the isentropic compression. However, the shock heating effect in stiff materials which do not undergo crystallographic phase changes is usually neglected at pressures up to about 500 kbar. For example, the temperatures of shocked MgO[13] with an initial temperature of 20°C are estimated to be 102°C at 247 kbar and 212°C at 493 kbar.

III. Production of plane shock waves

Because of the one-dimensionality of basic shock relations, meaningful property measurements in shock wave experiments can only be made in a one-dimensional planar geometry. The explosive plane wave lens can produce plane wave detonation fronts and essentially one-dimensional planar shock fronts in samples. The Snell's-law plane wave lens[14] consists of a conical shell of higher-velocity explosive and a cone of lower-velocity explosive, as shown in Fig. 2. A half of the vertical angle θ is chosen so that the vertical component of the higher detonation velocity D_h is equal to the lower detonation velocity D_l, or

$$\theta=\cos^{-1}(D_l/D_h)\,. \tag{5}$$

(13) T.J. Ahrens, J. appl. Phys., **37** (1966), 2532.
(14) W.B. Benedick, Rev. sci. Instr., **36** (1965), 1309.

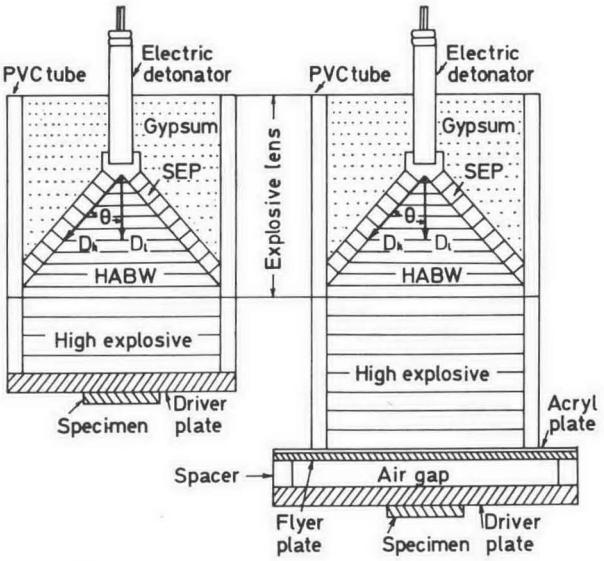

Fig. 2(a) Fig. 2(b)

Fig. 2. Devices for production of plane shock wave
(a) In-contact method (b) Flyer method

Two clay-like plastic explosives, SEP and HABW, containing a high explosive substance PETN (pentaerythritol-tetranitrate), manufactured by Asahi Chemical Industry Co., Ltd., are used for the higher and lower velocity explosives, respectively. Approximate compositions are as follows: SEP (65% PETN, 35% binder); HABW (30% PETN, 50 % Pb_3O_4, 20 % binder). By means of the so-called ion gap method the detonation velocities of SEP and HABW are determined to be 6.67 mm/μs and 5.05 mm/μs, respectively. Thus the angle θ is chosen to be 40°51′. The diameter of the explosive lens used in the present study is 40 mm, 51 mm or 78 mm, being much smaller than a usual one. It is to be emphasized that the smallest explosive lens weighs only 40 g.

Using a brass mold shown in Fig. 3, the plastic explosive SEP is shaped into a conical shell in a gypsum cast in a PVC (polyvinyl-chloride) cylinder. Then, a cone of HABW which is also shaped using a similar brass mold is inserted to fit the conical shell of SEP. During the molding process, a care is taken so as to introduce no void in the clay-like explosives.

The plane shock wave produced by the explosive lens is transmitted to a specimen mounted on a driver plate in contact with a high explosive pad, which is inserted between the explosive lens and the driver plate for the purpose of intensifying the shock pressure. This method, called the in-contact method, is shown in Fig. 2(a). The high explosive pad, 20 mm or 30 mm thick, is composed of Octol, Composition B, Pentolite, Baratol, or SEP in order to produce various values of the shock pressure. Various in-contact plane wave generator systems and values of

pressure produced in the driver plate are listed in Table 1. The shock pressure produced in the specimen is determined by the characteristic of high explosive and the shock impedances ($\rho_0 U$) of both the specimen and the driver material. Generally the value of pressure in the specimen is not equal to that in the driver plate. The highest pressure obtained by the in-contact method is about 400 kbar.

Higher shock pressures can be realized by the impact of an explosive-driven flyer plate upon the driver plate[15], as shown in Fig. 2(b). An acrylite plate about

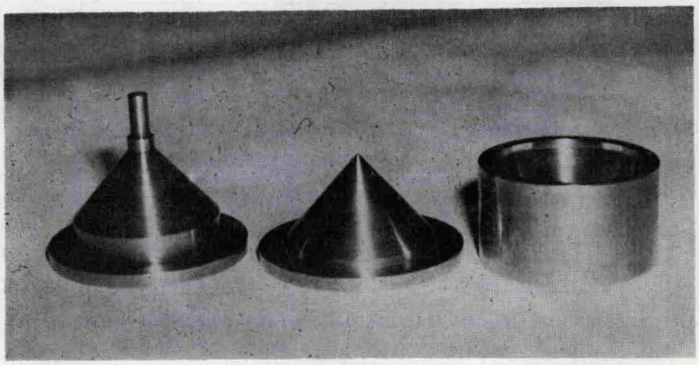

Fig. 3. Brass molds for making the explosive plane wave lens

Table 1. In-contact plane wave generator systems

Explosive lens diameter	High explosive pad (thickness)	Driver plate (thickness)	Shock pressure in driver plate
40 mm	SEP (20 mm)	Brass (3.5 mm)	160 kbar
	Pentolite (20 mm)	Brass (3.5 mm)	300 kbar
	Octol (20 mm)	Brass (3.5 mm)	300 kbar
51 mm	SEP (20 mm)	2024Al (5 mm)	120 kbar
		Brass (5 mm)	160 kbar
	Pentolite (20 mm)	2024Al (5 mm)	230 kbar
		Brass (5 mm)	300 kbar
	Comp. B (30 mm)	2024Al (5 mm)	290 kbar
		Brass (5 mm)	340 kbar
	Octol (30 mm)	2023Al (5 mm)	310 kbar
		Brass (5 mm)	410 kbar
78 mm	SEP (30 mm)	2024Al (5 mm)	120 kbar
		Brass (5 mm)	160 kbar
	Baratol (30 mm)	2024Al (5 mm)	140 kbar
		Brass (5 mm)	190 kbar
	Pentolite (30 mm)	2024Al (5 mm)	230 kbar
		Brass (5 mm)	300 kbar
	Comp. B (30 mm)	2024Al (5 mm)	290 kbar
		Brass (5 mm)	340 kbar
	Octol (30 mm)	2024Al (5 mm)	310 kbar
		Brass (5 mm)	410 kbar

(15) R.G. McQueen and S.P. Marsh, J. appl. Phys., **31** (1960), 1253.

Table 2. Flyer-plate plane wave generator systems

Explosive lens diameter	High explosive pad (thickness)	Flyer plate (thickness)	Driver plate (thickness)	Shock pressure in driver plate
51 mm	Pentolite (40 mm)	Brass (2.5 mm)	Brass (5 mm)	390 kbar
		Brass (2.0 mm)	Brass (5 mm)	500 kbar
		Brass (1.5 mm)	Brass (3 mm)	610 kbar
		Brass (1.0 mm)	Brass (3 mm)	770 kbar
78 mm	Pentolite (60 mm)	Brass (3.0 mm)	Brass (5 mm)	500 kbar
		Brass (2.0 mm)	Brass (5 mm)	670 kbar
		Brass (1.5 mm)	Brass (3 mm)	770 kbar
		Brass (1.0 mm)	Brass (3 mm)	900 kbar

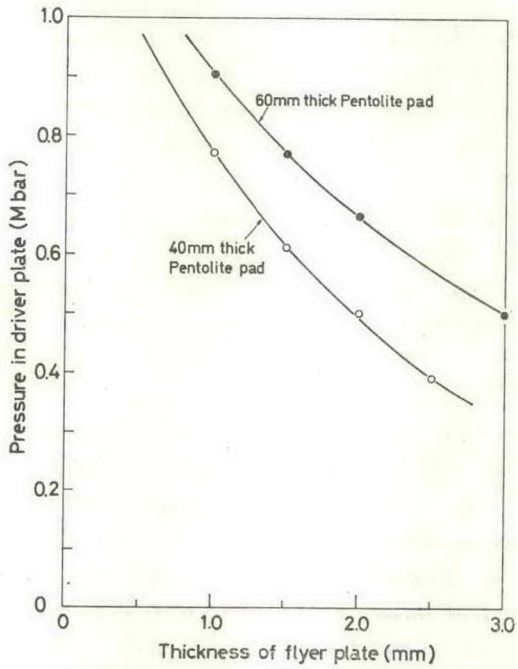

Fig. 4. Shock pressure in the brass driver plate produced by the impact of brass flyer plate

1 mm thick is inserted between the explosive pad and the flyer plate to protect the latter against the breakup during free flying. Various flyer-plate plane wave generator systems and values of pressure produced in the brass driver plate are listed in Table 2. The shock pressure in the brass driver plate is plotted against the thickness of the brass flyer plate in Fig. 4. The maximum pressure amounts to about 1 Mbar. The flyer method, however, gives worse planarity of the shock wave than the in-contact method. The planarity or the simultaneity of the shock arrival time has been examined by means of the argon flash gap technique

described in the next section (cf. Fig. 6). The in-contact method gives the planarity of ± 20 ns over 80 per cent of the diameter of the explosive lens. The planarity in the case of the flyer method depends on the flying distance, which must be less than 10 mm to obtain sufficient planarity for practical use. On the other hand, the flying distance must be large enough for the flyer plate to attain a uniform zero-pressure state after the shock acceleration by explosives; the distance corresponding to about 1/5 of the explosive thickness may be the lower limit.

IV. Determination of shock compression curve

As described in section II, a series of measurements of shock and free surface velocities determine the Hugoniot equation of state of a material. When the shock wave is incident on a free surface, the surface is very rapidly accelerated to a velocity u_f. Since the rise time to a peak pressure in the shock wave is normally very short, the time of the first motion of the free surface can be determined precisely. A time interval between the first motions of two different free surfaces gives the velocity of the shock propagated between them. If the subsequent displacement of the free surface is measured as a function of time, the free surface velocity is determined. Since only short times of 0.1–1 μs are available for these velocity measurements, the time resolution of the order of 10 ns is required for any recording system. The recording is made by either the electrical pin-contactor method or the optical streak-photographic method.

1. *Pin-contactor method*

The pin-contactor method[16] is the simplest technique for detecting the shock wave arrival at the free surface. The shock compression study of TiO_x[8] was made with this technique. A schematic representation of the pin arrangement for a metallic specimen such as TiO_x is indicated in Fig. 5(a). If the specimen is non-metallic, coaxial self-shorting pins are used instead of bare pins. The arrival of the shock front at the rear surface of the driver plate is recorded on a synchroscope by shorting of an electric circuit between the grounded driver plate and the rear pin A. Electric pulse signals generated by the electrical contact between the ground and the pins (B, B′ or C, C′), which are accurately positioned at known distances from the driver plate or the specimen, are also recorded to determine the shock transit time and the free surface travelling time of the driver material or the specimen, respectively. The surface pin B or C is positioned at a distance of 0.15 mm from the respective free surface to avoid the effect of the elastic precursor wave[16]. The distance between the other pin B′ or C′ and the respective free surface is limited within 2–3 mm in order to avoid the effect of multiple reflection of shock or rarefaction waves. A trigger pin T is also used to make sure of recording the pin signals on the synchroscope.

(16) S. Minshall, J. appl. Phys., **26** (1955), 463.

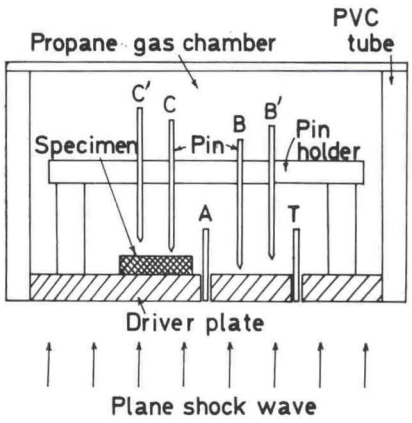

Fig. 5(a)

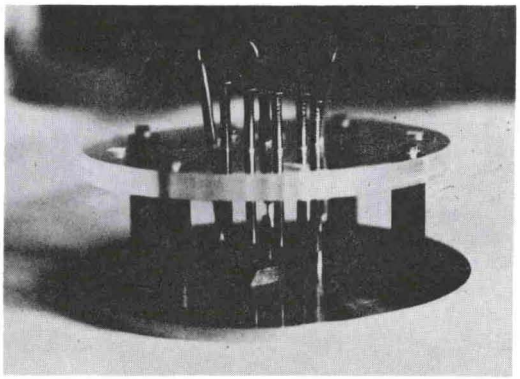

Fig. 5(b)

Fig. 5. Experimental set of the pin-contactor technique for measuring the shock and free surface velocities
(a) Schematic cross-sectional view (b) Photograph (Specimen: TiO_x)

Pin setting is performed by inserting standard block gages as a spacer between the pin and the free surface. A photograph of the experimental set is shown in Fig. 5(b). The precision of pin distances is estimated to be ± 0.01 mm. The precision of time interval measurements is limited mainly by the planarity of the shock wave front. It is important to avoid premature shorting of pins by shock ionization of air. Propane gas is flowed into a gas chamber to prevent it. A pulse forming circuit composed of fast switching diodes is used to obtain sharp pulse signals from the pin-contactors. Since the whole event is completed within a few μs, the sweeping speed of the synchroscope is chosen to be 0.5 μs/div or 0.2 μs/div, so that the time is detected with a precision of 10 ns.

Shock compression curves of TiO_x (x=0.84, 1.06 and 1.28) determined at pressures up to 600 kbar were described in ref. 8, together with an example of the synchroscope record of pin signals. It is to be mentioned here that TiO_x containing plenty of vacancy sites is rather incompressible even in this ultrahigh pressure region; no evidence is found for significant filling of vacancies.

2. *Streak-photographic method*

A streak-photographic method provides more reliable and informative data on the shock wave than the pin-contactor method. A rotating-mirror streak camera with a high frequency synchronous motor, was manufactured by the workshop in our institute. Details of this camera was described in a previous paper[17]. In this camera, an object is viewed through a slit, whose image is swept in an orthogonal direction by a rectangular flat rotating mirror. Thus the film records a one-dimensional space vs. time plot. The writing speed is 3–10 mm/

(17) J. Nakai, T. Goto, Y. Syono and Y. Nakagawa, Sci. Rep. RITU, A**25** (1975), 173.

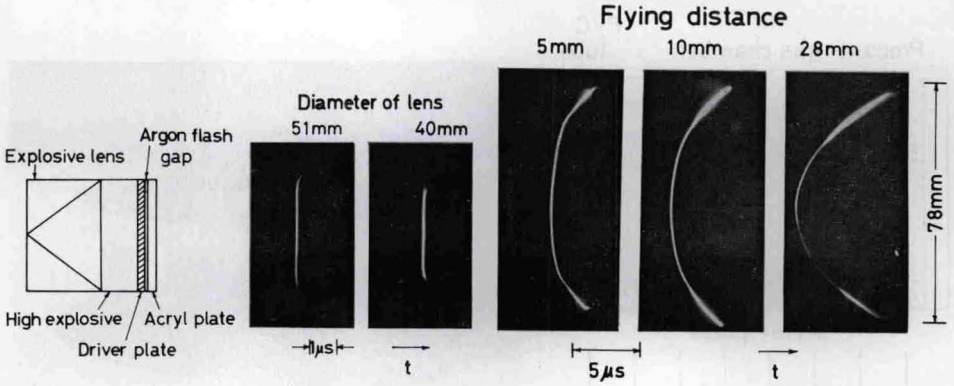

Fig. 6(a) Fig. 6(b)

Fig. 6. Planarity of the plane shock wave generators
(a) In-contact method (b) Flyer method
The flyer plate 78 mm in diameter and 3 mm thick is propelled by 30 mm thick Pentolite pad

μs, depending on the revolution of the rotating mirror. The time resolution is approximately 10 ns at best. A combination of two photographic camera lenses (an objective lens of f=300 mm, F4.5 and a relay lens of f=50 mm, F2) gives almost an equal size image of an object on the film at a distance of about 5 m. Using this streak camera, the following two techniques have been tried for the shock compression study.

1) *Argon flash gap technique*

One of the simplest optical method to detect the shock arrival is to utilize a brilliant light flash generated by shock-heated argon gas confined in a small gap. The argon flash gap technique is quite useful for the test of planarity of the plane wave generators shown in Fig. 2. Instead of the specimen, an acrylite plate is placed on the driver plate. A gap of about 0.1 mm between the acrylite plate and the driver plate is filled with argon of atmospheric pressure. The shock arrival gives rise to the motion of the driver plate which closes the gap, resulting in an emission of brilliant light. The light is viewed with the streak camera through a narrow slit; film records are shown in Fig. 6. Lines on the photographs exhibit the planarity of the plane wave generators: the in-contact method gives excellent results, while the flyer method is rather unsatisfactory, especially, in the case where the flying distance is large, as already mentioned in Section III.

An experimental set for the Hugoniot measurement using the argon flash gap technique[12),(15)] is illustrated in Fig. 7. Specimens and acrylite blocks are assembled in a direction across the diameter of the driver plate and viewed through the slit of the streak camera. Each acrylite block is covered with an iron shim of 0.1 mm in thickness made of a piece of thin razor blade, as shown in Fig. 8. The gap filled with argon gas between the acrylite block and the iron shim is separated

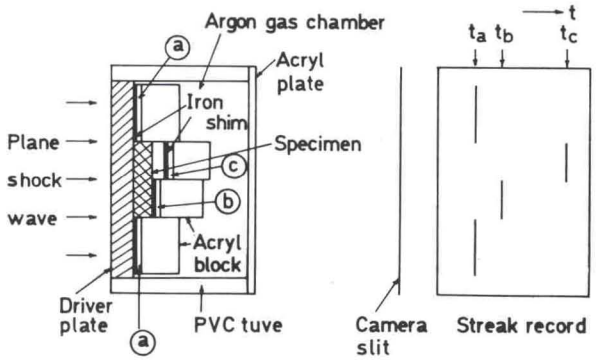

Fig. 7. Schematic view of the experimental set for measuring the shock and free surface velocities by means of the argon flash gap technique

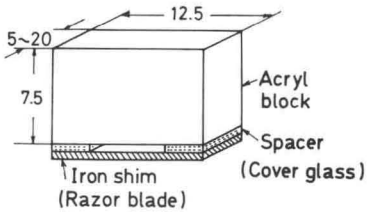

Fig. 8. Acrylite flash gap block (Dimension: mm)

by a thin glass spacer of 0.15 mm in thickness (a cover glass for optical microscopy). The incidence of the strong shock wave on the iron shim causes the gap to close, compressing and heating the gas to brilliant luminosity which is sufficient for exposure of the film in the streak camera as also illustrated in Fig. 7. The time of arrival of the shock wave on the surface of the driver plate, t_a, or that of the specimen, t_b, is detected with the argon flash gap labelled ⓐ or ⓑ, respectively. The shock velocity in the specimen can be calculated from $t_a - t_b$. The free surface velocity of the specimen is measured with the argon flash gap labelled ⓒ, which is positioned at a known distance from the free surface and becomes luminous at the time t_c. The accurate positioning of the acrylite block with a precision of 0.01 mm is performed using standard block gages as a spacer.

An example of streak records for the study on shock compression of Fe_3O_4[9] using both the in-contact method and the flyer method is shown in Fig. 9(a). A photograph of experimental sets used in a similar study on shock compression of GaP[10] is shown in Fig. 9(b). In each experiment, the planarity of the shock wave is monitored by three acrylite blocks located directly on the driver plate which becomes luminous at the time t_a. Three corresponding flash lines in each photographic record are quite straight for the in-contact run, whereas they are considerably curved for the flyer run. Other flash lines in the record correspond to the times t_b, t_c etc. These times must be corrected by taking the incomplete planarity into consideration. Broad flashes of light, which is clearly seen after the flash lines of argon gap in the record for the flyer run, are caused by the luminosity of argon gas behind the acrylite blocks which are moved by the collision of the specimen or the driver plate. In the record for the in-contact run, however, the broad flashes can scarcely be seen.

2) *Inclined mirror technique*

Since the argon flash gap technique provides only discrete information about

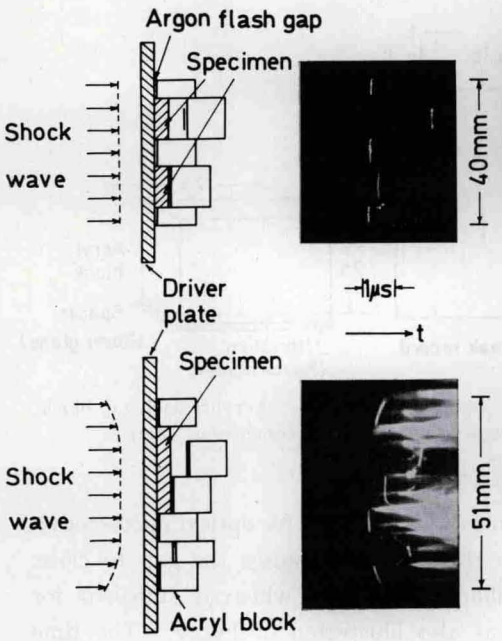

Fig. 9(a)

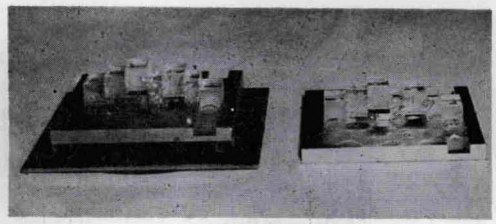

Fig. 9(b)

Fig. 9. Argon flash gap experimental sets and records
(a) Streak records (Specimen: Fe_3O_4)
Upper figure: in-contact method
Lower figure: flyer method
(b) Photograph of the experimental sets (Specimen: GaP)

time, its use is limited to cases where the free surface velocity is constant with time, i.e. the structure of shock wave is simple. A multiple shock wave such as the one resulting from phase transitions can be observed using another technique which allows the free surface motion to be monitored continuously. The inclined mirror technique[11], shown in Fig. 10(a), has been adopted as a simple continuous method.

This technique is based on the instantaneous change in reflectivity of a silvered glass mirror which takes place upon arrival of the shock wave. Some mirrors silvered on their inside surfaces are placed in contact with the driver plate or the specimen. Another mirror on the specimen surface is inclined at a small angle α. The assembly is illuminated by an intense light source such as a diffuse explosive argon candle and viewed through the slit of the streak camera. The sample chamber should be evacuated in order to avoid air shocks which perturb the mirror prior to the collision of the sample.

An example of the photographic record for the test sample of Fe is shown in Fig. 10(a). The arrival of the plane shock wave at the free surface of the sample is indicated by the decrease in intensity of the light reflected from the two mirrors in contact with the surface. A good planarity of the shock wave is clearly seen in the record. The free surface velocity of the sample is monitored by the point of collision of the sample with the inclined mirror, which is indicated by a trace of slanted image with an angle γ on the film. The free surface velocity is given by the following equation:

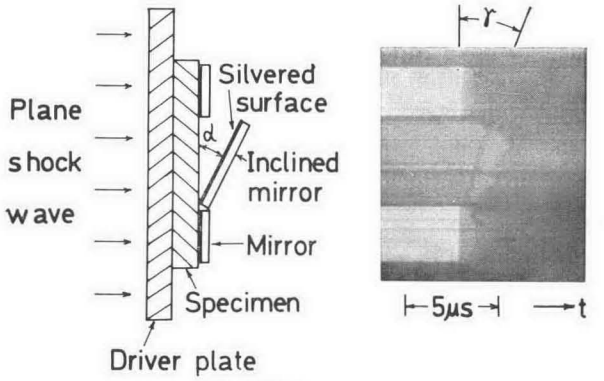

Fig. 10(a)

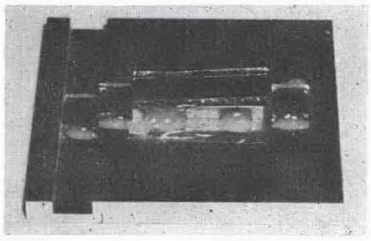

Fig. 10(b)

Fig. 10. Inclined mirror technique for measuring the free surface velocity
(a) The experimental set and its streak record (Specimen: Fe)
(b) Photograph of the experimental set (Specimen: GaAs)

$$u_f = W \tan \alpha / M \tan \gamma \,, \tag{6}$$

where W and M are the writing speed and the magnification of the streak camera, respectively. The inclined mirror technique is sensitive to the planarity of the shock wave front, and so it has been used only with the in-contact plane wave generator.

Figure 10(b) shows an experimental set for the study on shock compression of GaAs[10], in which the multiple shock wave due to the phase transformation is expected. The dimension of the sample is about 12 mm×25 mm×3 mm. The inclined mirror is set with an angle of about 3°30′, which is measured with a precision of ±2′.

If a double shock wave has passed through the specimen, the streak record must show a kink in the free surface trace, as shown schematically in Fig. 11. The slopes of the first and second traces correspond to the free surface velocities due to the first and second waves, respectively. The shock and free surface velocities of the first and second waves are given by the following equations:

$$U_1 = d/(t_1 - t_0) \tag{7a}$$

$$u_{f1} = W \tan \alpha / M \tan \gamma_1 \tag{7b}$$

$$U_2 = d + u_{f1}(t_2 - t_1)/(t_2 - t_0) \tag{8a}$$

$$u_{f2} = W \tan \alpha / M \tan \gamma_2 \,, \tag{8b}$$

where d is the thickness of the specimen, t_0 is the time of incidence of shock wave into the sample, t_1 and t_2 are the arrival times of two successive shock waves on the free surface of the specimen. Here, the subscripts 1 and 2 correspond to the first and second waves, respectively. On the basis of the free surface approximation, particle velocities are obtained from free surface velocities, i.e. $u_{f1}=2u_1$, $u_{f2}=2u_2$. Shock pressures and densities of the sample, (P_1, ρ_1) and (P_2, ρ_2), correspond-

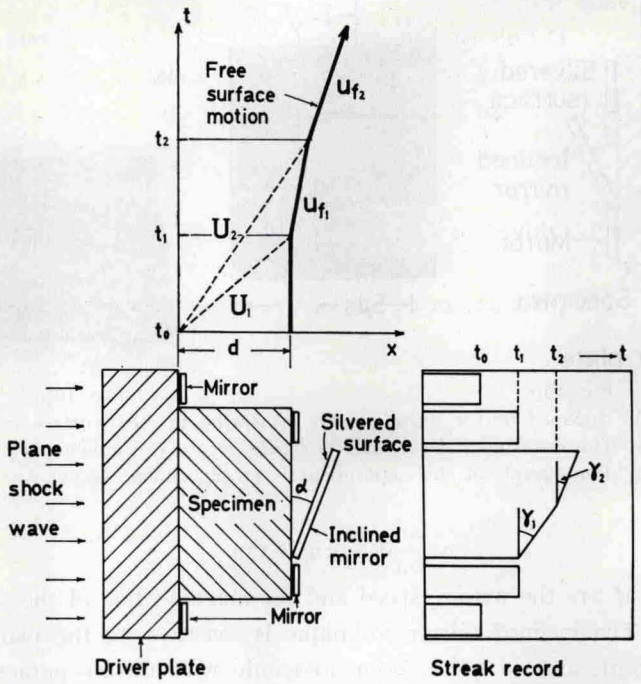

Fig. 11. Schematic illustration of an inclined mirror experimental record for a double shock wave

ing to the states (u_1, U_1) and (u_2, U_2) are given by the following equations which are easily derived from eqs. (1) and (2):

$$P_1 = \rho_0 U_1 u_1 \tag{9a}$$

$$\rho_1 = \rho_0 U_1/(U_1 - u_1) \tag{9b}$$

$$P_2 = P_1 + \rho_1 (U_2 - u_1)(u_2 - u_1) \tag{10a}$$

$$\rho_2 = \rho_1 (U_2 - u_1)/(U_2 - u_2)\,. \tag{10b}$$

Using both the argon flash gap technique and the inclined mirror technique, shock compression experiments have been performed for Fe_3O_4[9], αFe_2O_3[9] and GaAs[10]. An inclined mirror record for Fe_3O_4 catches a double shock wave structure associated with a high-pressure phase transition. Its pressure is determined to be 220 ± 20 kbar, which is slightly lower than that obtained by static high pressure experiments[18]. For αFe_2O_3, on the other hand, no evidence for phase transition is found at pressures up to about 500 kbar. Inclined mirror experiments of GaAs at 220 and 262 kbar exhibit three distinct waves: an elastic precursor wave and a double shock wave associated with a phase transition occurring at high pressure. From the analysis of the records, the Hugoniot elastic

(18) H.K. Mao, T. Takahashi, W.A. Bassett, G.L. Kinsland and L. Merill, J. geophys. Res., **79** (1974), 1165.

limit and the phase transition point are estimated to be 84 ± 8 kbar and 203 ± 11 kbar, respectively. Details of these data have been given in ref. (9) and (10). Measurements on resistivity of transition metal oxides under very high shock pressure have also been made and described in ref. (9).

V. Summary

In the present study, small-scale explosive plane wave generators 40–78 mm in diameter have been developed to perform shock wave experiments at pressures up to 1 Mbar. The planarity of the shock wave front has been tested with a high-speed streak camera: the in-contact method gives the planarity of ±20 ns over the 80 per cent of the diameter of the generator, while the planarity in the flyer method is worse than that in the in-contact method by a factor of 10.

Several experimental sets and techniques are used in the present investigation: the pin-contactor method is the simplest technique for measuring the shock and free surface velocities with usual synchroscope, and the streak-photographic method is a standard technique to obtain reliable and informative data on the equation of state. Among various streak-photographic methods, the argon flash gap technique and the inclined mirror technique are utilized to obtain shock compression curves of some materials.

Acknowledgments

The present authors are indebted to Mr. H. Moriya and Miss Y. Fujita for their assistance. Their thanks are due to members of the workshop who manufactured the experimental devices used in the present study. The present work was supported by the Grant-in-Aid for Scientific Research from the Ministry of Education.